Available online at www.sciencedirect.com
ScienceDirect
Biomaterials 28 (2007) 4209–4218
Biomaterials
www.elsevier.com/locate/biomaterials

# Biological performance in goats of a porous titanium alloy–biphasic calcium phosphate composite

JiaPing Li[a,b,e,*], Pamela Habibovic[a], Huipin Yuan[a], Mirella van den Doel[c], Clayton E. Wilson[b], Joost R. de Wijn[a], Clemens A. van Blitterswijk[a], Klass de Groot[a,d]

[a]*Institute for Biomedical Technology, University of Twente, The Netherlands*
[b]*Porogen B.V, The Netherlands*
[c]*Cellcotec B.V, The Netherlands*
[d]*CAM Implants B.V, The Netherlands*
[e]*School of Mechanical Engineering and Automation, BeiHang University, China*

Received 16 March 2007; accepted 29 May 2007
Available online 5 July 2007

**Abstract**

In this study, porous 3D fiber deposition titanium (3DFT) and 3DFT combined with porous biphasic calcium phosphate ceramic (3DFT + BCP) implants, both bare and 1 week cultured with autologous bone marrow stromal cells (BMSCs), were implanted intramuscularly and orthotopically in 10 goats. To assess the dynamics of bone formation over time, fluorochrome markers were administered at 3, 6 and 9 weeks and the animals were sacrificed at 12 weeks after implantation. New bone in the implants was investigated by histology and histomorphometry of non-decalcified sections. Intramuscularly, no bone formation was found in any of the 3DFT implants, while a very limited amount of bone was observed in 2 BMSC 3DFT implants. 3DFT + BCP and BMSC 3DFT + BCP implants showed ectopic bone formation, in 8 and 10 animals, respectively. The amount of formed bone was significantly higher in BMSC 3DFT + BCP as compared to 3DFT + BCP implants. Implantation on transverse processes resulted in significantly more bone formation in composite structure as compared to titanium alloy alone, both with and without cells. Unlike intramuscularly, the presence of BMSC did not have a significant effect on the amount of new bone either in metallic or in composite structure. Although the 3DFT is inferior to BCP for bone growth, the reinforcement of the brittle BCP with a 3DFT cage did not negatively influence osteogenesis, osteoinduction and osteoconduction as previously shown for the BCP alone. The positive effect of BMSCs was observed ectopically, while it was not significant orthotopically.


*Keywords:* Porous Ti6Al4V; Biphasic calcium phosphate (BCP); BMSC; Osteoconduction; Osteogenesis

## 1. Introduction

Bone grafts and bone graft substitutes are essential for replacement and repair of damaged and degraded skeletal tissue. Classical methods for bone repair employ autografts and allografts, which have good osteoinductive and osteoconductive properties. However, their use is often associated with important drawbacks such as limited availability and possible donor site morbidity for autografts [1,2] and disease transmission and immunologic incompatibility for allografts [3]. Synthetic bone graft substitutes, the design of which is based on mimicking the mineral composition of bone such as hydroxyapatite (HA), tricalcium phosphate (TCP) and biphasic calcium phosphate (BCP) ceramics, also possess satisfying bone healing properties. However, these materials are usually very stiff and brittle, have low impact resistance and relatively low tensile strength [4]. In large bone defects, which are unable to heal spontaneously, it is important to restore the structural integrity of the bone, as well as its function (i.e. load-bearing capacity) in as short as possible period of time. Due to poor mechanical properties of the

*Corresponding author. Institute for Biomedical Technology, University of Twente, Prof. Bronkhorstlaan 10-D, 3723MB Bilthoven, The Netherlands. Tel.: +31 30 2295289; fax: +31 30 2280255.
*E-mail address:* j.li@tnw.utwente.nl (J. Li).

0142-9612/$ - see front matter © 2007 Elsevier Ltd. All rights reserved.
doi:10.1016/j.biomaterials.2007.05.042

above-mentioned bone fillers their application in critical-sized bone defects is often associated with the simultaneous use of some kind of external fixation. In order to decrease the patient's discomfort during the healing process, ideally, bone fillers should be able to temporarily take over the mechanical function of the bone.

Metals possess mechanical properties suitable for load-bearing applications. However, the high stiffness of the metals often leads to stress shielding from the residual bone, which may result in detrimental resorptive bone remodeling, and consequently to a poor fixation of the implant. Recent developments in metallic implant design therefore focus on adapting the mechanical properties of metals to those of biological systems by, for example, applying a porous structure whereby mechanical interlocking may enhance the integration process.

Porous titanium and titanium alloys are of interest as they have been shown to possess excellent mechanical properties as permanent orthopedic implants under load-bearing conditions [5,6]. As titanium is a corrosion resistant but biologically inert material, different approaches to improve the response of bone to titanium have been investigated. Fujibayashi et al. [7] used chemical and thermal treatments for this purpose; Habibovic et al. [8] applied biomimetic octacalcium phosphate (OCP) coating to improve the osteoconductive and osteoinductive properties of porous titanium; Vehof et al. [9,11] and van den Dolder et al. [10] performed different studies in which they attempted to improve the biological properties of porous titanium mesh by combining scaffolds with either osteogenic cells or osteogenic growth factors.

In this present study, we produced composite structures consisting of 3D fiber deposition Ti6Al4V (3DFT) inside of which BCP ceramic was placed. The goal of this study was to investigate whether bone ingrowth inside metallic implants can be improved by the presence of bioactive ceramic in its center, improving implant fixation. In addition, we combined these implants with autologous bone marrow stromal cells (BMSCs).

3DFT was produced by rapid prototyping [12], a method that allows for fabrication of precisely defined porous structures, which is important as it has previously been reported that changing in scaffold geometry may affect the surrounding cells and tissue ingrowth [13,14]. Highly interconnected porous structures provide a large surface area, enabling cells to migrate, proliferate and differentiate [15,16]. The in-house produced BCP ceramic had a highly interconnected macro- and microporous structure, and was previously shown to be both osteoconductive and osteoinductive [17–20].

## 2. Materials and methods

### 2.1. Experimental design

This study, for which 10 Dutch milk goats were used, was approved by the Utrecht University animal care committee (DEC, Utrecht University, Utrecht, The Netherlands).

BMSCs were obtained, culture expanded and cryopreserved. Ten days before surgery the cells were thawed, allowed to acclimate for 3 days, seeded on 3DFT and 3DFT + BCP scaffolds and cultured in osteogenic medium. Bare scaffolds and the constructs with autologous BMSCs were implanted ectopically in the paraspinal muscles. Orthotopically, polymeric cages containing three conditions were implanted bilaterally on the L4 and L5 transverse processes according to a randomized complete block design (Fig. 1). To monitor bone formation over time, fluorochrome markers were administered at 3, 6 and 9 weeks and the animals were sacrificed at 12 weeks after implantation. Bone formation was investigated by histology and histomorphometry of non-decalcified sections using epifluorescent and light microscopy.

### 2.2. Implants

*3DFT*: Porous Ti6Al4V scaffolds were made by 3D fiber deposition as described earlier [12]. In short, Ti6Al4V slurry (80 wt% of powder Ti6Al4V in 0.5% aqueous water methylcellulose solution) is forced by gas pressure through a syringe nozzle of a 3D-bioplotter machine (Envisiontec GmbH, Germany). The slurry is deposited on a stage as a fiber, which rapidly solidifies by drying, and the scaffold is fabricated by layering a 0–45° pattern of fibers. After deposition, the obtained Ti6Al4V scaffolds were dried for 24 h at room temperature, and sintered under high vacuum at 1200 °C for 2 h. Both the fiber diameter and the space between fibers were around 400 μm. The compressive strength of thus produced 3DFT was higher than that of cancellous bone, and the Young's modulus value lied between that of cancellous and cortical bone. The permeability was comparable to that of cancellous bone [21]. The scaffolds were machined into the following implants: blocks with dimensions $4 \times 7 \times 8\,mm^3$ (metal alone) and $4 \times 7 \times 8\,mm^3$ with an inner hole of $4 \times 4 \times 4\,mm^3$ (composite) for orthotopic implantation, and blocks with dimensions of $4 \times 7 \times 8\,mm^3$ (metal alone) and $\varnothing 8 \times 8\,mm^2$ cylinders with a central hole of $\varnothing 5 \times 8\,mm^2$ for intramuscular implantation (Fig. 1).

For composite scaffolds porous BCP ceramic was prepared by using the so-called $H_2O_2$ method as published earlier [22]. For the preparation of the ceramic, in-house made BCP powder was used. Porous green bodies were produced by mixing this powder with 2% $H_2O_2$ solution (1.0 g powder/$1.2 \pm 0.05$ ml solution) and naphthalene (Fluka Chemie, The Netherlands) particles (710–1400 μm; 100 g powder/30 g particles) at 60 °C. The naphthalene was then removed by sublimation at 80 °C and the green porous bodies were dried. Finally, the bodies were sintered at 1200 °C for 8 h. Blocks with the dimensions of $4 \times 4 \times 4\,mm^3$ and cylinders of $\varnothing 5 \times 8\,mm^2$ were machined and fitted into relative 3DFT bodies to make the composites.

The microstructure of different implants was characterized by using an environmental scanning electron microscope (ESEM; XL30, ESEM-FEG, Philips, The Netherlands) in the secondary electron mode.

The BCP ceramic composition and crystal structure were determined by Fourier Transform Infra Red Spectroscopy (FTIR; Spectrum100, Perkin Elmer Analytical Instruments, Norwalk, CT) and X-ray Diffraction (XRD; Miniflex, Rigaku, Japan). HA/$\beta$-TCP weight ratio in the BCP was calculated by comparing the XRD pattern to the calibration patterns prepared from the powders with the known HA/$\beta$-TCP weight ratios. Each type of scaffold was left without or cultured with BMSCs. BMSC constructs were never placed next to unseeded scaffolds in the transverse process cages.

For intramuscular and orthotopic implantation, four types of implants were prepared:

1. 3DFT: 3DFT scaffolds without cells;
2. BMSC 3DFT: 3DFT scaffolds with cells;
3. 3DFT + BCP: 3DFT + BCP scaffolds without cells;
4. BMSC 3DFT + BCP: 3DFT + BCP scaffolds with cells.

### 2.3. Cages for orthotopic implantation on transverse processes

Cage design and fabrication were described previously [23]. The scaffolds, polyacetal components of the cages and the metal screws were sterilized by autoclaving. Three scaffolds ($4 \times 7 \times 8\,mm^3$) were plugged

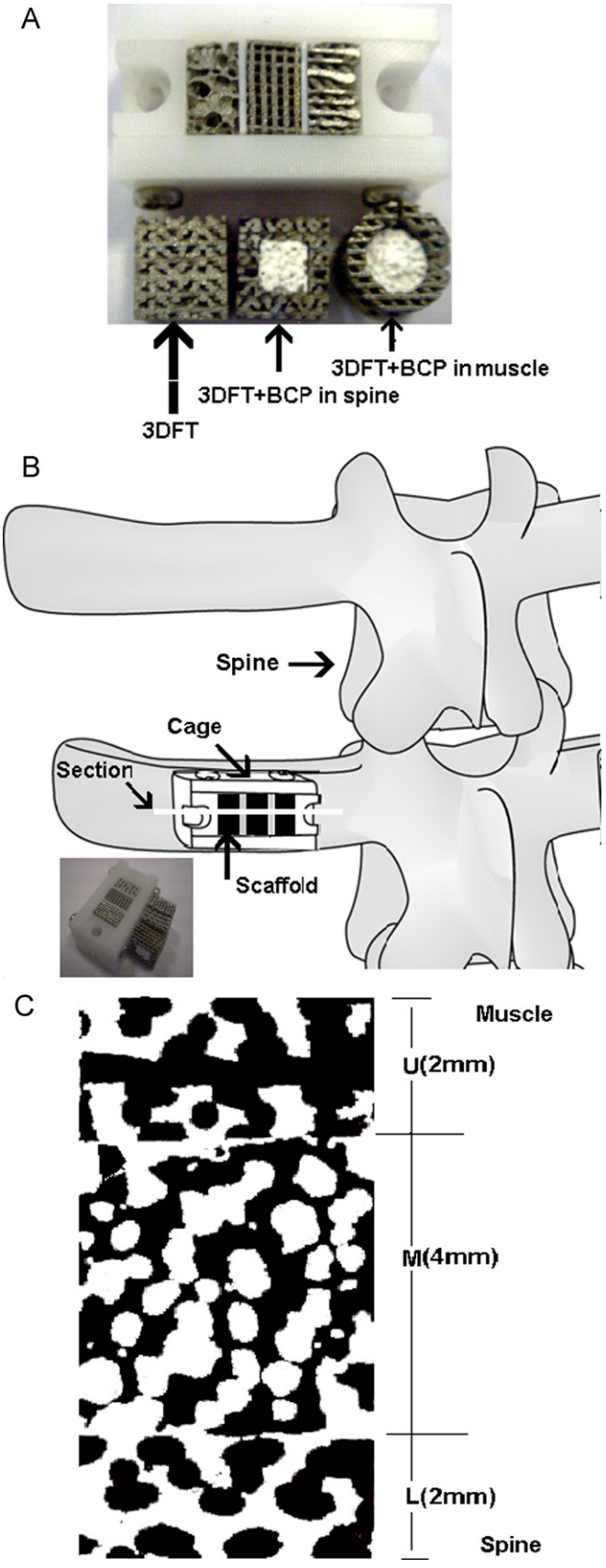


into a cage and separated by thin Teflon plates ($0.5 \times 7 \times 8\,mm^3$). Four spinal cages were implanted bilaterally on the transverse processes of the L4 and L5 vertebrae of each goat according to a randomized complete block design. In addition to the four conditions that are discussed in this paper, another eight Ti alloy conditions were evaluated the findings of which will be presented separately. The orthotopic scaffolds were open to both the underlying bone and the overlying soft tissues. Implants and cage are shown in Fig. 1.

### 2.4. BMSC culture and seeding conditions

Autologous serum (AS) was derived from 100 ml venous blood that was taken at the time of bone marrow aspiration [24]. The BMSCs were derived from 30 ml bone marrow obtained from the iliac wings of each goat according to a previously described procedure [25]. The cells were cultured for 7–10 days in standard culture medium containing 15% of fetal bovine serum (FBS, Gibco, Paisly, Scotland) [26]. Medium containing non-adherent cells was removed after 2–3 days and replaced by fresh medium. Cells were then trypsinized and concentrated by centrifugation at 1500 rpm for 4 min followed by resuspension in 10 ml of fresh medium containing 30% FBS and 10% dimethylsulfoxide (DMSO, Sigma, The Netherlands) for cryopreservation. Ten days before surgery, the cells were thawed in pure FBS, centrifuged at 1500 rpm for 4 min and after washing with culture medium, re-plated in medium containing 10% FBS. After 3 days of culture, cells were washed with PBS, then detached and centrifuged before resuspension at a concentration of $5 \times 10^6$ cells/ml in medium containing 15% AS. BMSCs scaffolds per goat were immersed in 4 ml of this suspension respectively, and incubated for 2 h. After the cell-seeding period, each construct was placed in a well of a 25-well plate. The constructs were pre-cultured for 1 week under static conditions in 3 ml of medium containing 15% AS and 10 mM $\beta$-glycerophosphate (BGP, Sigma, Zwijndrecht, The Netherlands) and 10 nM dexamethasone (DEX, Sigma).

The control scaffolds (without cells) were placed in the same medium for the same period of time as the BMSCs constructs. The medium was changed every 2–3 days. At the end of the incubation period, implants were transported to surgery in serum-free medium.

### 2.5. In vitro analysis of implants

Two implants of each implant type were used to determine cell proliferation and viability by Alamar blue assay at days 1, 4 and 6. The Alamar blue solution was diluted 1:10 in culture medium, and the constructs were cultured for 2 h. Then, 200 µl of Alamar blue solution from each well was transferred into 96-well plates, and fluorescence was measured using a Perkin Elmer Luminescence Spectrometer LS50B. Results were recorded by FL Winlab software.

### 2.6. Implantation

Ten adult Dutch milk goats ($\pm$2 years old), weighing 45–75 kg (mean weight: $65 \pm 8.5$ kg), were housed at the Central Animal Laboratory Institute (GDL), Utrecht, The Netherlands, at least 4 weeks prior to surgery.

The surgical procedures were performed under standard conditions [19,23]. After shaving and disinfection of the dorsal thoracolumbar area, a midline skin incision from T8–L5 was made to expose the paraspinal muscles that were separated longitudinally to expose the transverse

Fig. 1. (A) Implants for intramuscular and spinal implantation. (B) Schematic drawing of spinal cage mounted on a transverse process. The lower left is the position of three implants in a cage. (C) Central slide through 3DFT + BCP. Division of the implant area on histological sections as used for histomorphometry for studying bone ingrowth from host bone bed. The implant was classifiled three parts: the upper (U) quarter, middle (M) half and lower (L) quarter (in the composite structures these lines separate different materials).

processes of the L4 and L5 vertebrae. The processes were decorticated using an angled bone rasp. One cage was screwed to each process. Finger pressure was applied to the top of the blocks in the cage prior to muscle closure to ensure direct contact of all blocks with the underlying bone. After spinal cage implantation, using blunt dissection, separate intramuscular pockets were created in the T8–L3 paraspinal muscles and filled with one of the intramuscular conditions according to a randomized scheme. Subsequently, the fascia was closed with a non-resorbable suture to facilitate implant localization at explantation. The skin was closed in two layers. Durogesic 25 (fentanyl transdermal CII patches; Janssen-Cilag EMEA, Beerse, Belgium) was administered for postoperative pain relief.

Sequential fluorochrome markers were administered at 3 weeks (CalceinGreen, 10 mg/kg, Sigma, The Netherlands), 6 weeks (Oxytetracyclin, Engemycine 32 mg/kg, Mycofarm, The Netherlands) and 9 weeks (Xylenol Orange, 80 mg/kg Sigma) in order to visualize bone growth dynamics.

At 12 weeks, the animals were euthanized by an overdose of pentobarbital (Organon, Oss, The Netherlands). Spinal cages were retrieved by sawing off the transverse processes, while intramuscular implants were removed with some surrounding muscle tissue.

### 2.7. Histological processing and histomorphometry

The explanted samples were fixed in a solution of 5% glutaraldehyde and 4% paraformaldehyde at 4 °C. Fixed samples were dehydrated by ethanol series (70–100%) and transferred into a methylmethacrylate (MMA) solution that polymerized at 37 °C within 1 week. Three centrally located longitudinal 10–15-μm-thick sections were cut from each sample using a sawing microtome. Two sections were stained with 1% methylene blue and 0.3% basic fuchsin after etching with HCl/ethanol mixture for histology. The third section remained unstained for epifluorescence microscopy of the fluorochrome markers.

Implanted materials were qualitatively analyzed using a light microscope (E600 Nikon, Japan). The presence of fluorochrome markers were evaluated using a light/fluorescence microscope (E600, Nikon, Japan) equipped with a quadruple filter block (XF57, dichroic mirror 400, 485, 558 and 640 nm, Omega Optics, The Netherlands). High-resolution digital scans of the stained sections of spinal cage implants were made for histomorphometry using a photographic film scanner (Dimage Scan Elite 5400, Minolta, Japan). Prior to histomorphometrical analysis, bone and material were pseudocoloured, red and green respectively, by using Adobe Photoshop 6.0. Image analysis was performed using a PC-based system with the KS400 software (version 3, Zeiss, Germany). Prior to measurements the system was geometrically calibrated with an image of a block of known dimensions to analysis the area of implant. A custom-made macro was developed to measure area of interest, area of scaffold, area of bone, scaffold outline available for bone apposition, contact length of bone and scaffold [13]. The following parameters were investigated:

1. The percentage of bone area in total available pore space (%b. pore total), in the low quarter of the implant (%b. pore low), in the middle half of the implant (%b. pore middle, M area in Fig. 1C; only applicable for orthotopic implantation) and in the upper quarter of the implant (%b. pore upper, U area in Fig. 1C; only applicable for orthotopic implantation).
2. %b. cont. total: percentage of length of contact between bone and scaffold outline relative to total available scaffold outline in the total implant area: [(bone contact scaffold length/scaffold outline length) × 100%].

### 2.8. Statistics

Statistical calculations were performed with the SPSS 14.0 software (Chicago, IL). We found large variances in the amount of bone between individual animals and the data obtained from histomorphometry were not normally distributed in all cases. That is why we chose the non-parametric Friedman signed-rank test for paired comparisons, followed by a *post hoc* test to compare the four implant types from the spinal implantation site. As only two types of implants showed bone formation intramuscularly, the non-parametric Wilcoxon signed rank test for paired comparisons was used to perform the statistical analysis.

For both tests, the significance level was set at $p = 0.05$.

## 3. Results

### 3.1. Material characterization and in vitro results

XRD and FTIR analysis confirmed the biphasic nature of the BCP ceramic, consisting of 80 ± 5% HA and 20 ± 5% β-TCP (data not shown). Macro- and microstructures of 3DFT and 3DFT + BCP implants are shown in Fig. 2. As observed by the ESEM, 3DFT implants consisted of a well-interconnected macroporous structure, with a pore size of around 400 μm. The porosity of 3DFT was 55 ± 3%. BCP scaffolds also possessed an interconnected macroporous structure with pore sizes varying between 100 and 800 μm. The porosity of BCP was 60 ± 4%. At high magnification micropores (pore size $<10$ μm) became visible in the structure of both scaffolds, 3DFT and BCP (Fig. 2C and D). Results of Alamar blue assay on days 1, 4 and 6 are shown in Fig. 3. Between days 1 and 4, an increase in cellular activity for all implant types was observed, suggesting cell proliferation or possibly an increased cell metabolism per individual cell. After day 4, leveling off in cellular activity suggested the short of differentiation or possibly decreased metabolism due to oxygen limitation. At days 1 and 4, metabolic activity on metal alone was lower than on BCP containing implants; this difference disappeared after 6 days of culture.

### 3.2. In vivo results

#### 3.2.1. Intramuscular implantation

At retrieval, all implants were surrounded by well-vascularized muscle tissue. Histology showed no indications for toxicity of the implants nor was there any signs of an inflammatory tissue response directly related to the implants observed. Table 1 shows bone incidence in different implants after 12 weeks of intramuscular implantation. None of the bare titanium alloy implants showed bone formation. They were filled with fibrous tissue containing capillaries, and occasionally showed fatty tissue in-growth (Fig. 4A). Two of the BMSC 3DFT implants showed bone formation albeit to a limited extend (Fig. 4B). In one of these implants the xylenol orange fluorochrome label was observed, indicating that bone was formed between sixth and ninth week of implantation (data not shown). In the other implant, none of the labels was found, suggesting that the start of bone formation had taken place after 9 weeks. In both composite structures, bone was only observed in the pores of the BCP ceramic, rather than in the titanium alloy area of the implant. While in 3DFT + BCP implants, bone was found in eight out of 10 animals, the composite structure with BMSCs showed

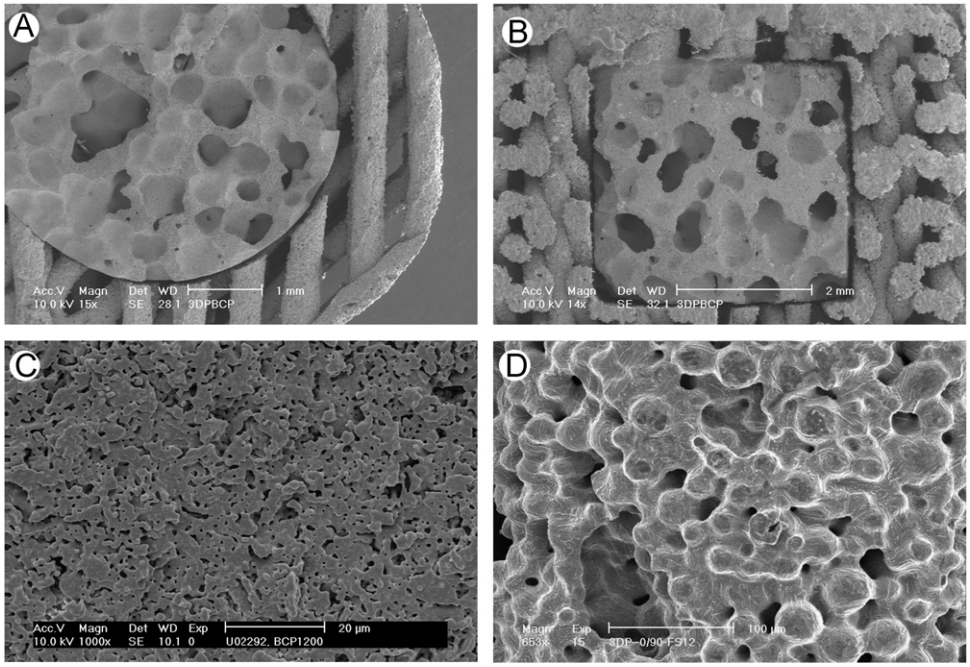


Fig. 2. ESEM photographs of the scaffolds. Macrostructure of composite structure implants for intramuscular (A) and orthotopic (B) implantation and microstructure of BCP (C) and 3DFT surface (D).

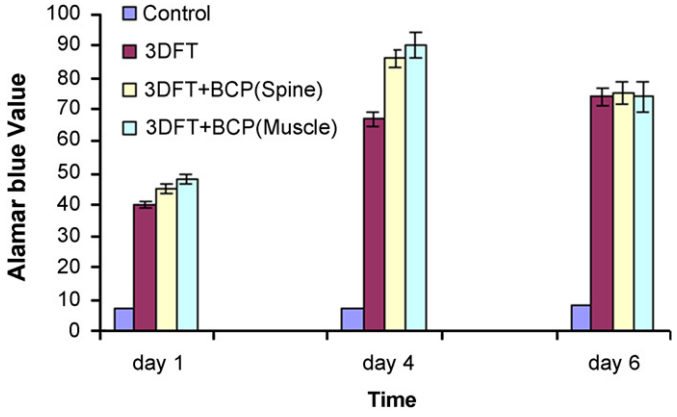


Fig. 3. Alamar blue value for different implant types at 1, 4 and 6 days of culture. Up to 4 days, increased metabolism is observed, after which it is levelled off.

bone formation in all animals. All three fluorochrome markers were found in BMSC 3DFT + BCP implants suggesting an early start of bone formation before the third week of implantation. Histomorphometrical analysis of the amount of bone formed in the available pore area indicated significantly more bone formation in BMSCs 3DFT + BCP as compared to 3DFT + BCP ($p = 0.003$, Fig. 5). Similar results were obtained for bone contact measurements (data not shown).

### 3.2.2. Orthotopic implantation

Upon explantation, no macroscopic or microscopic signs of infection were found. All cages were found firmly attached to the underlying transverse processes, even after removing the bone screws. In all implants, bone ingrowth started from the host bone bed towards the implant. New bone did not completely fill any of the implants, so the final amount of bone in the implants could be used for measuring the effect of various implants to new bone formation. In the 3DFT and BMSC 3DFT, bone formation was obviously the result of ingrowth from the underlying bone (osteoconduction) as in both 3DFT and BMSC 3DFT bone was predominantly found in the lower part of the implants adjacent to the underlying transverse processes (Fig. 6A and C). In contrast to 3DFT implants, in both 3DFT + BCP and BMSC 3DFT + BCP implants, bone had reached the top of the middle part of the implant (Fig. 6B and D).

Histomorphometrical analysis confirmed the histological observations revealing that a relatively low amount of bone was formed in 3DFT and BMSC 3DFT implant (about 2–3% of the total implant area was new bone). Significantly more bone was found in 3DFT + BCP and BMSC 3DFT + BCP implants (about 8–10% of total implant area). Fig. 7 represents histomorphometrical data of bone area in the available pore space of the total implant. 3DFT + BCP, as well as BMSC 3DFT + BCP showed significantly more bone area than both 3DFT ($p = 0.01$ and $p < 0.001$, respectively) and BMSC 3DFT ($p = 0.005$ and $p < 0.001$, respectively). No significant difference was found between either 3DFT and BMSC 3DFT or between 3DFT + BCP and BMSC 3DFT + BCP. As can be observed, the general phenomenon is that the amount of bone was dependent on the presence of BCP rather than on the presence of cells. Similar significant differences as those for bone area in available pore space were also found for the

Table 1
Bone incidence intramuscular in goat

| Implant | Bone incidence after 12 weeks |
|---|---|
| 3DFT | 0/10 |
| BMSC 3DFT | 2/10 |
| 3DFT + BCP | 8/10 |
| BMSC + 3DFT + BCP | 10/10 |

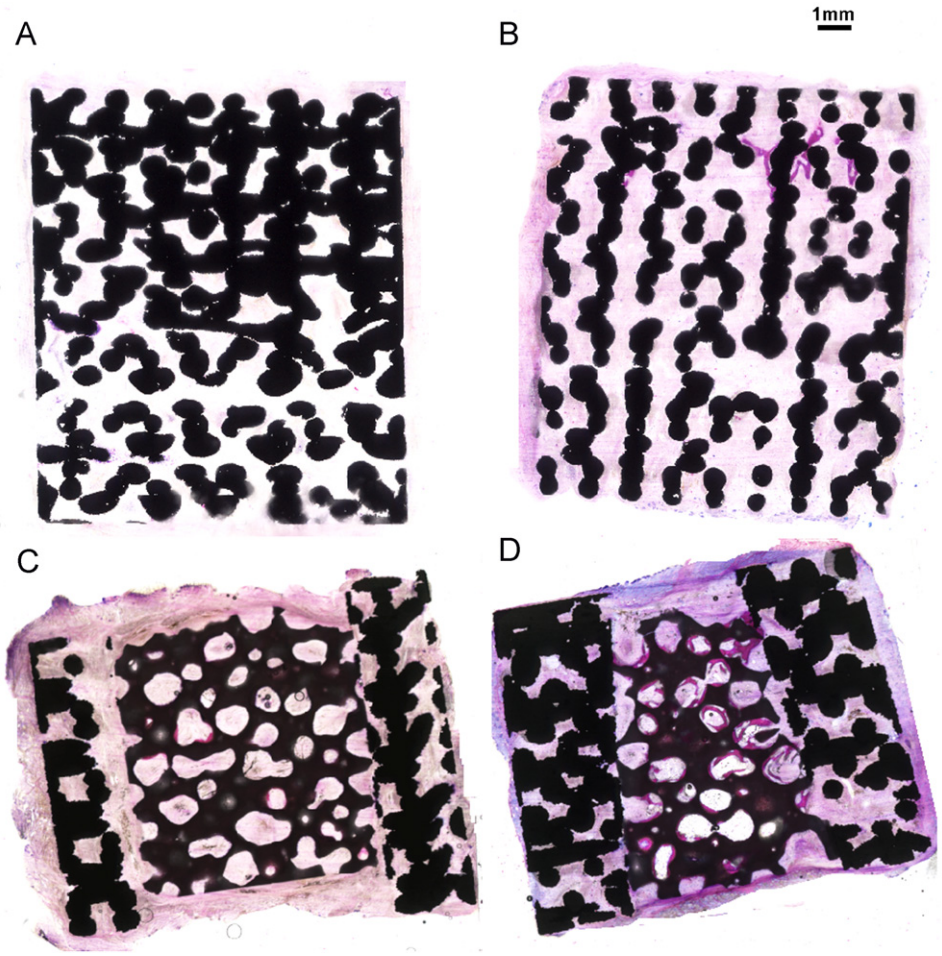


Fig. 4. Digital photographs of stained (methylene blue/basic fuchsine) histological sections of 3DFT (A), BMSC 3DFT (B), 3DFT + BCP (C) and BMSC 3DFT + BCP (D) implants after 12 weeks of implantation in paraspinal muscles.

measured bone contact (Fig. 8). Regarding the bone ingrowth into different areas of implants in the available pore space, no significant difference was found between different implant types (Fig. 9A) in the quarter of the implant closest to the host bone bed (L area in Fig. 1C). Logically, the bone area in the middle half of both 3DFT + BCP and BMSC 3DFT + BCP (M area in Fig. 1C) was significantly larger as compared to the implants consisting of metal alone clearly demonstrating difference in bioactivity between Ti alloy and BCP ceramic (Fig. 9B). No bone formation was found in the upper part of implant (U area in Fig. 1C).

Fluorescent microscopy of the sequential fluorochrome labels revealed the dynamics of bone formation in different implants. In most implants, all three labels were present in the lower part of implants, closest to transverse process as is illustrated by BMSC 3DFT + BCP micrograph in Fig. 10A, suggesting the start of new bone formation before the third week of implantation. In the middle part, all three markers were also found in the BMSC 3DFT + BCP implants (Fig. 10B), unlike for the other implant types, suggesting an osteogenic effect of the cells. In the middle half of the 3DFT + BCP implants, only the oxytetracycline (6-week) and xylenol orange (9-week)

markers were observed, while there were no markers in 3DFT and BMSC 3DFT implants, confirming the histological observation of lack of bone formation in the deeper regions of metallic implants. Another remarkable observation was that in the middle part of 3DFT + BCP and BMSC 3DFT + BCP implants, early fluorochrome markers were observed predominantly on the interface between Ti alloy and BCP.

## 4. Discussion

In this *in vivo* study in goats, we investigated the behavior of 3DFT metallic implants and 3DFT + BCP composite structure either as such or as constructs loaded with autologous BMSCs by implanting them in paraspinal muscles and on lumbar transverse processes. The goal of the study was to combine BCP and 3DFT to make benefit of the advantageous characteristics of both materials [8]. By incorporating BCP inside a 3DFT cage, optimal bioactivity of the ceramics was combined with optimal biomechanical characteristics of the porous metal. BCP ceramic was chosen for the preparation of composite implants, since previous animal studies have shown that this material has a high osteoinductive and osteoconductive potential and is appropriate for cell-based bone formation [17,27].

As we did not find signs of foreign body reaction related to the implants, we can conclude that 3DFT and 3DFT + BCP have an acceptable biocompatibility to be used as bone graft substitute.

Intramuscularly, no bone formation was observed in 3DFT implants, while only two out of 10 implants showed

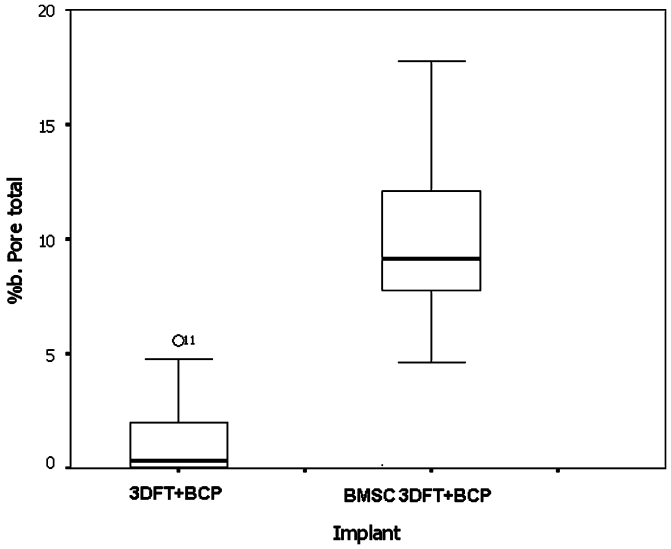


Fig. 5. Histomorphometrical results: boxplots (mean and interquartile values) of bone formation in total available pore space in 3DFT + BCP and BMSC 3DFT + BCP implants after 12 weeks of intramuscular implantation. (“o” indicates outlier).

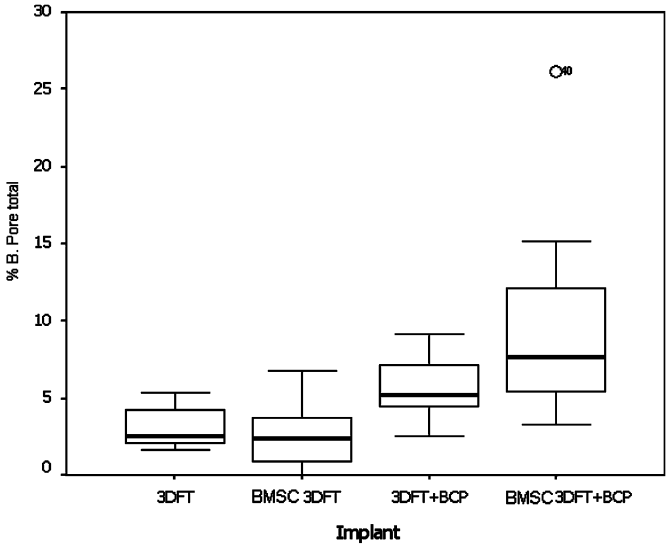


Fig. 7. Histomorphometrical results: boxplots (mean and interquartile values) of the percentage of new bone area in the total available pore space (region of interest) after 12 weeks of implantation on lumbar transverse process. (“o” indicates outliers).

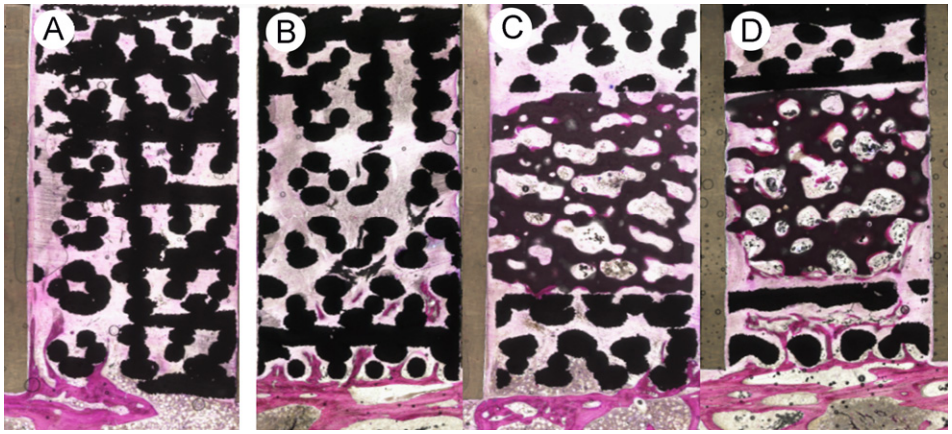


Fig. 6. Digital photographs of stained (methylene blue/basic fuchsine) histological sections of 3DFT (A), BMSC 3DFT (B), 3DFT + BCP(C) and BMSC 3DFT + BCP (D) after 12 weeks of implantation on lumbar transverse processes. Bone is stained pink/red, Ti alloy black and BCP ceramic dark brown. The transverse process can be seen at the bottom of the implants and Teflon plates are visible between the implants.

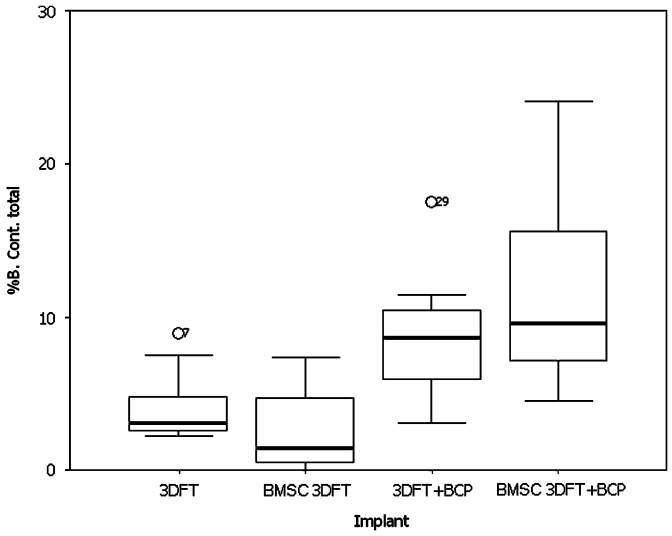


Fig. 8. Histomorphometrical results: boxplots (mean and interquartile values) of the percentatge of the total length of available scaffold outline in contact with bone in the total implant area ("o" indicates outliers).

a very limited amount of bone in BMSC 3DFT implants. In contrast to metallic implants, bone incidence in composite implants was 80% and 100% for 3DFT + BCP and BMSC 3DFT + BCP, respectively. The amount of bone formed in BMSC 3DFT + BCP implants was significantly higher as compared to bare composite implant.

The observed differences in bone formation between titanium alloy and titanium alloy combined with BCP ceramic can be explained by the well-known excellent bioactivity of BCP. In view of this, biphasic CaP ceramics, composed of HA and TCP, are considered to be even more bioactive than HA alone [19,28], possibly due to higher resorbability. Moreover, some BCP ceramics have been shown to induce ectopic bone formation without addition of osteogenic factors and to be able to heal clinically relevant critical-sized defects in goats [17,18,20] and rabbits [19]. Combined with a bone morphogenic protein (osteogenin), BCP ceramic has shown good results in the healing of a segmental defect in the rat long bone [18].

The difference in bone formation between 3DFT + BCP and BMSC 3DFT + BCP is most probably caused by the presence of osteogenic cells in BMSC construct. During the culturing of cells on the scaffolds in order to produce constructs for the implantation, BGF and DEX were added into culturing medium, which is suggested to stimulate osteogenic differentiation [29,30]. After 7 days of culture, the extracellular matrix was formed in the scaffolds. This extracellular matrix may be useful for bone formation as reported previously [26]. BMSC did have a significantly positive effect on ectopic bone formation when seeded on composite structure implants, and only a moderate effect on metallic implants. This might be explained by the difference in the interaction with cells and endogenous growth factors between the BCP and Ti6Al4V surface. This is conceivable, based on earlier

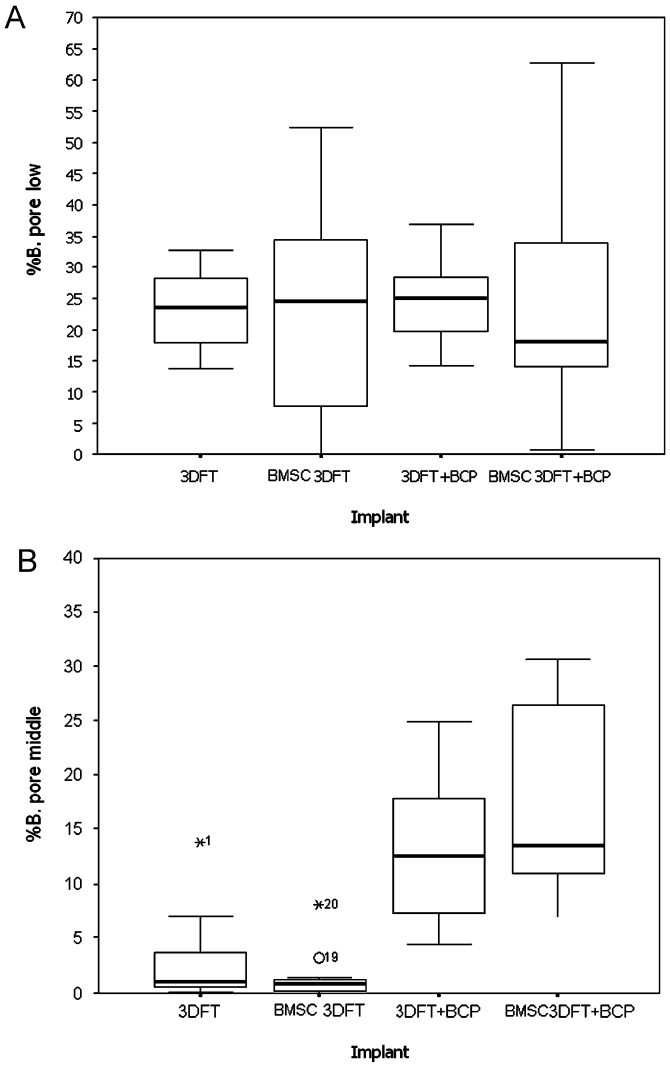


Fig. 9. Histomorphometrical results of bone area in the available pore space in (A) the quarter of the implant closest to transverse process (L area in Fig. 1C) and (B) the middle half of the implant (M area in Fig. 1C) ("o" and "x" indicate outliers and extreme outliers, respectively).

reports of favorable behavior of CaP ceramics due to preferential binding of growth factors and/or bone marrow cells to their surfaces [9,31,32]. Our results are in agreement with earlier studies with titanium fiber mesh in which more bone formation was shown when metallic implants were coated with calcium phosphate and loaded with cells [9,33].

Similar to intramuscular results, the presence of BCP ceramic had a significantly positive effect on bone formation at the orthotopic implantation site. Even though BCP ceramic was not in direct contact with either underlying bone of the transverse process or with the muscles covering the cage, its excellent bioactivity was apparent in both the amount and the rate of new bone formation.

Unlike intramuscularly, BMSC did not have a significant effect on orthotopic bone formation in either metallic or in composite implants although there are indications for cell derived (early) osteogenesis as is shown by the presence of

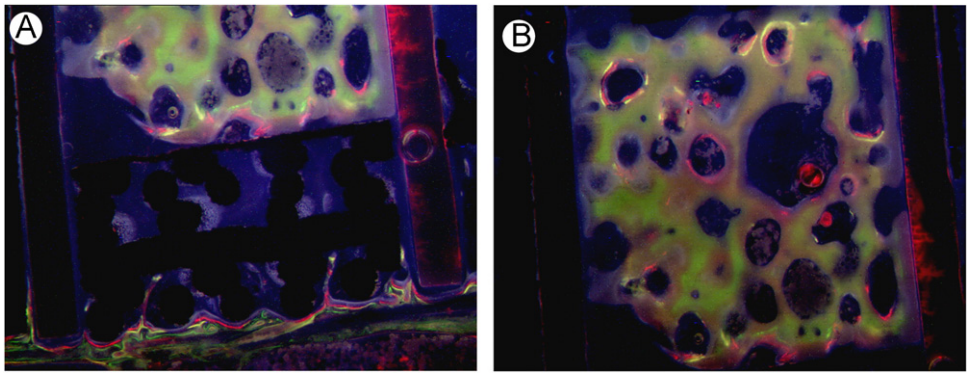


Fig. 10. Epifluorescent microscopy images of fluorochrome markers in the low part of implant (A) and BCP part (B) of BMSC 3DFT + BCP implant after 12 weeks of implantation on lumbar transverse process. In all images the earliest label is green (3 weeks, calcein green), the middle label is yellow (6 weeks, oxytetracycline) and the final label is orange (9 weeks, xylenol orange).

early fluorochrome markers in the middle of BMSC 3DFT + BCP implants. This observation is in accordance with a previous study of the effect of orthotopic BCP tissue-engineered constructs in goats [20]. A few reasons can be given as possible explanation for the lack of effect of tissue engineering orthotopically. In the study, the surface of transverse process was removed by a rasp. The resultant surgical trauma unavoidably caused primary mechanical damage to the vasculature, cells, matrix and bone marrow, possibly resulting in impaired circulation, exudates and hemorrhage. Taken that the success of tissue engineering for a large part lies in the communication of the implanted cells with its surroundings, damage caused by the surgical procedure may be the reason for the poor effect of tissue engineering on the implants on the transverse processes as compared to intramuscular implantation, where the surgical trauma is much less severe.

Another possible reason for the lack of the effect of tissue engineering orthotopically may be the effect of the endogenous cells. It is well known that stromal stem cells exist in the bone marrow, and under specified conditions can proliferate and differentiate into osteoblastic cells, resulting in the formation of bone [34–36]. Perhaps, in combination with the materials with high osteoconductive and osteoinductive potential such as BCP ceramic, the effect of endogenous cells and growth factors is strong enough to overrule that of the implanted cells, in particular after a longer implantation time. Although we could not find differences in the amount of formed bone between BMSC 3DFT + BCP and 3DFT + BCP implant, the fluorochrome labels showed that BMSC 3DFT + BCP induced earlier start of bone formation than 3DFT + BCP. Similar observations of the temporary effect of tissue engineering when appropriate osteoconductive/ostoinductive implants are used has been reported previously [20]. A better understanding of the processes involved in the osteogenicity of tissue-engineered constructs is needed to give the exact explanation of the results observed in our study.

Another interesting observation of this study was that in composite implants early fluorochrome labels (calcein green or oxytetracycline) often appeared on the interface between BCP and titanium alloy both on the side of overlying muscle and underlying bone, rather than in the middle of the BCP part. This is likely the result of oxygen supply and nutrient diffusion from the host tissues, as it is well known that bone only forms early in the presence of vasculature which has to come from the muscle or the underlying bone [17]. In the middle part, the lack of nutrient delivery and waste removal delayed the bone growth. In other words, the preferential location for the start of new bone formation was in the first place determined by the bioactivity of the surface (BCP rather than Ti alloy) and in the second place by the oxygen and nutrients supply (periphery of the BCP part the implants rather than its center).

## 5. Conclusion

In the current study, 3DFT and 3DFT + BCP scaffolds, bare and seeded with goat BMSC were implanted intramuscularly and orthotopically in 10 goats. The results showed that when a titanium alloy cage was placed around a biphasic BCP scaffold, the osteoconductive, osteoinductive and osteogenic properties of the ceramic were not negatively affected. Therefore, this kind of composite may be useful for reconstruction of large loaded bone defects as it provides the mechanical stability of the metal while retaining the bioactivity of the ceramic. In addition, the results of this study indicated that the composition of the implant, i.e. the presence of the bioactive ceramic had a more significant effect on the biological performance of the investigated implants than the presence of autologous osteogenic cells.

## Acknowledgments

Authors would like to thank Dr. Maarten Terlou from the Image Analysis Department of the Utrecht University for developing the software used for the histomorphometry and Dr. Moyo Kruyt for fruitful discussions. This study

was for a part financially supported by CAM Implants B.V., Leiden, The Netherlands.

## References


[1] Damien CJ, Parsons JR. Bone graft and bone graft substitutes: a review of current technology and applications. J Appl Biomater 1991;2(3):187–208.

[2] Arrington ED, Smith WJ, Chambers HG, Bucknell AL, Davino NA. Complications of iliac crest bone graft harvesting. Clin Orthop Relat Res 1996;329:300–9.

[3] Brantigan JW, Cunningham BW, Warden K, McAfee PC, Steffee AD. Compression strength of donor bone for posterior lumbar interbody fusion. Spine 1993;18(9):1213–21.

[4] Rezwan K, Chen QZ, Blaker JJ, Boccaccini AR. Biodegradable and bioactive porous polymer/inorganic composite scaffolds for bone tissue engineering. Biomaterials 2006;27(18):3413–31.

[5] Ryan G, Pandit A, Apatsidis DP. Fabrication methods of porous metals for use in orthopaedic applications. Biomaterials 2006;27(13): 2651–70.

[6] Crowninshield RD. Mechanical properties of porous metal total hip prostheses. Instr Course Lect 1986;35:144–8.

[7] Fujibayashi S, Neo M, Kim HM, Kokubo T, Nakamura T. Osteoinduction of porous bioactive titanium metal. Biomaterials 2004;25(3):443–50.

[8] Habibovic P, Li J, Van Der Valk CM, Meijer G, Layrolle P, Van Blitterswijk CA, et al. Biological performance of uncoated and octacalcium phosphate-coated Ti6Al4V. Biomaterials 2005;26(1):23–36.

[9] Vehof JW, Spauwen PH, Jansen JA. Bone formation in calcium-phosphate-coated titanium mesh. Biomaterials 2000;21(19):2003–9.

[10] van den Dolder J, Farber E, Spauwen PH, Jansen JA. Bone tissue reconstruction using titanium fiber mesh combined with rat bone marrow stromal cells. Biomaterials 2003;24(10):1745–50.

[11] Vehof JW, Mahmood J, Takita H, van't Hof MA, Kuboki Y, Spauwen PH, et al. Ectopic bone formation in titanium mesh loaded with bone morphogenetic protein and coated with calcium phosphate. Plast Reconstr Surg 2001;108(2):434–43.

[12] Li JP, de Wijn JR, Van Blitterswijk CA, de Groot K. Porous Ti6Al4V scaffold directly fabricating by rapid prototyping: preparation and *in vitro* experiment. Biomaterials 2006;27(8):1223–35.

[13] Tsuruga E, Takita H, Itoh H, Wakisaka Y, Kuboki Y. Pore size of porous hydroxyapatite as the cell-substratum controls BMP-induced osteogenesis. J Biochem (Tokyo) 1997;121(2):317–24.

[14] Jin QM, Takita H, Kohgo T, Atsumi K, Itoh H, Kuboki Y. Effects of geometry of hydroxyapatite as a cell substratum in BMP-induced ectopic bone formation. J Biomed Mater Res 2000;51(3):491–9.

[15] Chang BS, Lee CK, Hong KS, Youn HJ, Ryu HS, Chung SS, et al. Osteoconduction at porous hydroxyapatite with various pore configurations. Biomaterials 2000;21(12):1291–8.

[16] Du C, Meijer GJ, van de Valk C, Haan RE, Bezemer JM, Hesseling SC, et al. Bone growth in biomimetic apatite coated porous polyactive 1000PEGT70PBT30 implants. Biomaterials 2002;23(23): 4649–56.

[17] Habibovic P, Yuan H, van den Doel M, Sees TM, van Blitterswijk CA, de Groot K. Relevance of osteoinductive biomaterials in critical-sized orthotopic defect. J Orthop Res 2006;24(5):867–76.

[18] Habibovic P, Yuan H, van der Valk CM, Meijer G, van Blitterswijk CA, de Groot K. 3D microenvironment as essential element for osteoinduction by biomaterials. Biomaterials 2005;26(17): 3565–75.

[19] Kruyt MC, Wilson CE, de Bruijn JD, van Blitterswijk CA, Oner CF, Verbout AJ, et al. The effect of cell-based bone tissue engineering in a goat transverse process model. Biomaterials 2006;27(29): 5099–106.

[20] Kruyt MC, Dhert WJ, Yuan H, Wilson CE, van Blitterswijk CA, Verbout AJ, et al. Bone tissue engineering in a critical size defect compared to ectopic implantations in the goat. J Orthop Res 2004;22(3):544–51.

[21] Li JP, Wijn JR, Van Blitterswijk CA, De Groot K. Comparison of porous Ti6Al4V made by sponge replication and directly 3D fiber deposition and cancellous bone. Key Eng Mat 2007;330–332: 999–1002.

[22] Yuan H, Kurashina K, de Bruijn JD, Li Y, de Groot K, Zhang X. A preliminary study on osteoinduction of two kinds of calcium phosphate ceramics. Biomaterials 1999;20(19):1799–806.

[23] Wilson CE, Kruyt MC, de Bruijn JD, van Blitterswijk CA, Oner FC, Verbout AJ, et al. A new *in vivo* screening model for posterior spinal bone formation: comparison of ten calcium phosphate ceramic material treatments. Biomaterials 2006;27(3):302–14.

[24] Kruyt MC, de Bruijn JD, Wilson CE, Oner FC, van Blitterswijk CA, Verbout AJ, et al. Viable osteogenic cells are obligatory for tissue-engineered ectopic bone formation in goats. Tissue Eng 2003;9(2): 327–36.

[25] Kruyt MC, de Bruijn JD, Yuan H, van Blitterswijk CA, Verbout AJ, Oner FC, et al. Optimization of bone tissue engineering in goats: a peroperative seeding method using cryopreserved cells and localized bone formation in calcium phosphate scaffolds. Transplantation 2004;77(3):359–65.

[26] Kruyt MC, Dhert WJ, Oner C, van Blitterswijk CA, Verbout AJ, de Bruijn JD. Optimization of bone-tissue engineering in goats. J Biomed Mater Res B Appl Biomater 2004;69(2):113–20.

[27] Yang Z, Yuan H, Tong W, Zou P, Chen W, Zhang X. Osteogenesis in extraskeletally implanted porous calcium phosphate ceramics: variability among different kinds of animals. Biomaterials 1996; 17(22):2131–7.

[28] Kruyt MC, van Gaalen SM, Oner FC, Verbout AJ, de Bruijn JD, Dhert WJ. Bone tissue engineering and spinal fusion: the potential of hybrid constructs by combining osteoprogenitor cells and scaffolds. Biomaterials 2004;25(9):1463–73.

[29] Mendes SC, Tibbe JM, Veenhof M, Both S, Oner FC, van Blitterswijk CA, et al. Relation between *in vitro* and *in vivo* osteogenic potential of cultured human bone marrow stromal cells. J Mater Sci Mater Med 2004;15(10):1123–8.

[30] Mendes SC, Van Den Brink I, De Bruijn JD, Van Blitterswijk CA. *In vivo* bone formation by human bone marrow cells: effect of osteogenic culture supplements and cell densities. J Mater Sci Mater Med 1998;9(12):855–8.

[31] Ohgushi H, Goldberg VM, Caplan AI. Heterotopic osteogenesis in porous ceramics induced by marrow cells. J Orthop Res 1989;7(4):568–78.

[32] Ohgushi H, Goldberg VM, Caplan AI. Repair of bone defects with marrow cells and porous ceramic. Experiments in rats. Acta Orthop Scand 1989;60(3):334–9.

[33] Vehof JW, van den Dolder J, de Ruijter JE, Spauwen PH, Jansen JA. Bone formation in CaP-coated and noncoated titanium fiber mesh. J Biomed Mater Res 2003;64A(3):417–26.

[34] Buckwalter JA, Glimcher MJ, Cooper RR, Recker R. Bone biology. II: Formation, form, modeling, remodeling, and regulation of cell function. Instr Course Lect 1996;45:387–99.

[35] Haynesworth SE, Goshima J, Goldberg VM, Caplan AI. Characterization of cells with osteogenic potential from human marrow. Bone 1992;13(1):81–8.

[36] Chang Y-S, Gu H-O, Kobayashi M, Oka M. Influence of various structure treatments on histological fixation of titanium implants. J Arthroplast 1998;13(7):816–25.